



EUROfusion

EUROFUSION WPJET2-PR(16) 14834

Y Zhou et al.

Microanalysis of deposited layers in the divertor of JET with ITER-like wall

Preprint of Paper to be submitted for publication in
22nd International Conference on Plasma Surface Interactions
in Controlled Fusion Devices (22nd PSI)



This work has been carried out within the framework of the EUROfusion Consortium and has received funding from the Euratom research and training programme 2014-2018 under grant agreement No 633053. The views and opinions expressed herein do not necessarily reflect those of the European Commission.

This document is intended for publication in the open literature. It is made available on the clear understanding that it may not be further circulated and extracts or references may not be published prior to publication of the original when applicable, or without the consent of the Publications Officer, EUROfusion Programme Management Unit, Culham Science Centre, Abingdon, Oxon, OX14 3DB, UK or e-mail Publications.Officer@euro-fusion.org

Enquiries about Copyright and reproduction should be addressed to the Publications Officer, EUROfusion Programme Management Unit, Culham Science Centre, Abingdon, Oxon, OX14 3DB, UK or e-mail Publications.Officer@euro-fusion.org

The contents of this preprint and all other EUROfusion Preprints, Reports and Conference Papers are available to view online free at <http://www.euro-fusionscipub.org>. This site has full search facilities and e-mail alert options. In the JET specific papers the diagrams contained within the PDFs on this site are hyperlinked

Microanalysis of deposited layers in the divertor of JET with ITER-like wall.

Y. Zhou^a, H. Bergsaker^a, I. Bykov^a, P. Petersson^a, G. Possnert^b, J. Likonen^c, J. Pettersson^d, S. Koivuranta^c, A.M. Widdowson^e and JET contributors^f

EUROfusion Consortium, JET, Culham Science Centre, Abingdon, OX14 3DB, UK

*^aDepartment for Fusion Plasma Physics, School of Electrical Engineering,
Royal Institute of Technology, S-10405 Stockholm, Sweden*

^bUppsala Universitet, Tandem Laboratory, S-75105 Uppsala, Sweden

^cVTT Technical Research Centre of Finland, P.O.Box 1000, FIN-02044 VTT, Finland

^dDepartment of Chemistry – BMC, Uppsala Universitet, Box 599, 75124 Uppsala, Sweden

^fCCFE, Culham Science Centre, Abingdon, Oxon, OX14 3DB, UK

^eSee the Appendix of F. Romanelli et al., Proceedings of the 25th IAEA Fusion Energy Conference 2014, Saint Petersburg, Russia

Abstract.

In JET with ITER-like wall, beryllium eroded in the main chamber is transported to the divertor and deposited mainly at the horizontal surfaces of tiles 1 and 0 (high field gap closure, HFGC). These surfaces are tungsten coated carbon fibre composite (CFC). Surface samples were collected following the plasma operations in 2011-2012 and 2013-2014 respectively. The surfaces, as well as polished cross sections of the deposited layers at the surfaces have been studied with micro ion beam analysis methods (μ -IBA). Deposition of Be and other impurities, and retention of D is microscopically inhomogeneous. Impurities and trapped deuterium accumulate preferentially in cracks, pits and depressed regions, and at the sides of large pits in the substrate (e.g. arc tracks where the W coating has been removed). With careful overlaying of μ -NRA elemental maps with optical microscopy images, it is possible to separate surface roughness effects from depth profiles at microscopically flat surface regions.

Presenting and presenting author: Y. Zhou.

1. Introduction

Erosion of plasma facing components and materials migration limit the lifetime of the first wall in fusion devices [1]. In particular, the formation of thick deposited layers in wall areas with net deposition entails trapping of fuel by codeposition and the break up of thick deposits leads to undesired dust production [1]. The trapping of tritium fuel could pose a radiological problem in ITER and impair the fuel economy in a power producing plant (fusion reactors will critically depend on retrieving and breeding sufficient amounts of tritium). If more than one plasma facing material is used, materials mixing may modify the plasma surface interactions properties.

ITER is being built with beryllium plasma facing components in the main chamber and tungsten in the divertor. In preparation for ITER, the ITER-like wall experiments (JET-ILW) were set up at JET [2], with operations starting in 2011. In the main chamber, the plasma facing surfaces are mainly Be tiles, while in the divertor W coated carbon fibre composite (CFC) tiles are used, with the exception of the central Tile 5, which is made of bulk W. Compared to the previous all carbon conditions (JET-C), fuel trapping at divertor surfaces has been significantly reduced [3]. To determine precisely where net deposition takes place and where D (and T) is trapped, as well as other long term effects on the surfaces, it is necessary to extract surface samples for post mortem analysis. As previously in JET-C, this has been done following the first periods of operations with JET-ILW, 2011-2012 and 2013-2014. The analysis was mainly by microscopy, ion beam analysis (IBA), secondary ion mass spectrometry (SIMS) and thermal desorption analysis (TDS) [3-6]. Other techniques for Be analysis include accelerator mass spectrometry (for ^{10}Be marker) and inductively coupled plasma atomic emission spectroscopy (ICP-AES) [7]. In JET-ILW the thickest deposits of Be, originating from the main chamber wall, have been found on the horizontal upper part of Tile 1 in inner the divertor, and at Tile 0. [3,4]. This is also where more than 70% of the D trapped in the inner divertor is found [5,6].

The divertor surfaces in JET-ILW were comparatively rough already before operations started. Surface roughness from the fibre structure of the CFC is carried over through the coatings. Microscopically, following plasma operations there are also frequently pits and cracks in the coatings. It has long been observed that net deposition of impurities at plasma exposed rough surfaces can take place preferentially within pits, cracks, arc tracks and other depressed regions [8]. As a result, it has been reported that in an experiment with ^{13}C impurity marker, it accumulated 3-5 times faster at a rough surface, compared to smooth surfaces [9]. It is well established that fuel retention can likewise be enhanced within pits [10]. This was observed also in JET-C [11-13], where enhanced D concentration was found within deposits in pockets in the substrate [12] and inside cracks. Enhanced D content was found also within buried dust particles [12].

There are several reasons to study the microscopic distribution of impurity deposition and fuel trapping. Firstly, it is not quite clear why the distributions become non uniform, so further studies may improve understanding of the deposition mechanisms. Secondly, data have to be

extrapolated from the JET-ILW divertor with rough surfaces, to ITER with at least initially smooth surfaces; microanalysis may allow this step to be taken with more confidence. Thirdly, many broad beam IBA and other surface analysis methods with modest spatial resolution are difficult to interpret without microscopic information and microanalysis facilitates that interpretation. Finally, the assessment of many proposed fuel removal methods must surely be sensitive to whether fuel has been accumulated uniformly, or preferentially depending on surface roughness features.

Microanalysis of divertor surfaces from JET-ILW following the first shut down has been presented in [13-15]. Emphasis was on the vertical surfaces of Tiles 1 and 3 in the inner divertor, and Tiles 6-8 in the outer divertor. Non uniform impurity deposition and fuel retention was found in particular at the vertical surfaces in the inner divertor. In JET-ILW, not only was deposition enhanced within cracks and pits in the substrate, it was also frequently enhanced at specific slopes on the sides within larger pits [13,14]. This suggests that the microscopically local ion flux may play an important role, since it is likely to be asymmetric. That would call for modelling including the detailed ion gyro motion [16-18]. That assumption is supported by the finding that both in JET-C [12] and in JET-ILW [14] the direction of column growth in the deposited layers is in directions compatible with the local ion angle of incidence [18]. By restricting analysis to microscopically flat regions it was possible to establish that D had been trapped deep inside the W coatings, and at the W/Mo and Mo/W interfaces in coatings with marker layers, dominating the D retention in the outer divertor [15]. Using the same technique an upper bound could be determined to any Be/W mixing within the original W coating [15].

This report extends the analysis to the second shut down with JET-ILW. It also focuses on the upper part of Tile 1 and on Tile 0 (where previously no microanalysis had been made), i.e. where most of the Be deposition and D retention occurs.

2. Experimental

Samples were taken from the inner divertor tiles, Tile 0 (the High Field Gap Closure tile) and Tile 1 following operations 2011-2012 and 2013-2014. The positions of tiles and samples in the poloidal cross section of JET vessel are shown in Figure 1. On Tile 0, samples from four different toroidal positions were investigated. Samples were cut out with a coring technique at VTT in Otaniemi, Finland. A few of the samples were also cut perpendicularly to the surface and polished, so that the deposited layer cross sections could be examined. Each sample was marked, so that its original orientation in the vessel is known. The sample surfaces were investigated with optical microscopy and with micro ion beam analysis (μ -IBA) at the Tandem laboratory in Uppsala, Sweden [11-15]. Details about the experimental setup, quantification, data handling and presentation are best described in [13]. For this work 4.8 MeV ^3He beam was used to analyse the beryllium and deuterium in the deposited layers using the $\text{D}(^3\text{He},\text{p})^4\text{He}$ and $\text{Be}(^3\text{He},\text{p})^{11}\text{B}$ nuclear reactions. Protons were detected with an annular detector with 0.4 sr solid angle, situated at around 165° backward angle. The depletion layer of the detector is 1500 μm , thus sufficient to stop protons completely. Most of the time a 30 μm Al foil was used to stop backscattered ions in front of the detector. This geometry provides for negligible shadowing effects with a rough target and high sensitivity, while still

retaining sufficient energy resolution to allow depth profiles of D and Be to be determined. Before the measurements, copper grids (100M or 200M) were glued to the sample surface with epoxy to identify the areas of interest and to allow for comparison of the elemental maps with microscopic images. The Cu grids, as well as SS components, Mo and W were mapped from the characteristic X-rays (PIXE), using an Si(Li) X-ray detector at 45° with respect to the sample surface normal. This geometry is somewhat sensitive to shadowing effects with a rough surface. The X-ray yield from the Cu grids was used for beam current integration. The beam size, which defines the spatial resolution, was focussed to about 10 μm. Mapping data was stored as 256x256 spatial matrices.

Focus stacking was used in the optical microscopy. This allows for sharp pictures over a wide focal range and gives a possibility to determine the surface topography, in this work with about 4 μm resolution. The proton energyspectrawere analysed using SIMNRA [19].

3. Results

The horizontal tiles in the upper part of the inner divertor have significant toroidal assymetry due shadowing from adjacent tiles. Following the 2011-2012 operations, particularly at position 0/2 there were several deep arc tracks, either going perpendicularly to the magnetic field, or as small spots, where the W coating had been completely eroded. Figure 2 shows an example of elemental distribution in and around two such arc spots. The proton spectrum in the upper left panel shows how C, Be, superficial D and deeply trapped D can be separated. The upper right panel shows a topographic map of the surface. Besides the arc spot, there is a region with a valley in the substrate to the upper right. The rims of the spots, carrying molten W, rise about 20 μm above the surrounding W surface. The elemental maps, overlaid with optical micrographs, show that the carbon substrate is unveiled within the arc spots. This is also where most of the deposited Be and superficial D have accumulated. However, much of the deep D is found in the depressed region along the upper right hand side of the images. The fibre structure of the CFC substrate goes vertically, in this case parallel to the magnetic field, and some of that linear vertikal structure can be found in the deep D distribution.

Figure 3 shows elemental maps of a cross section of the W coating from the horizontal part of tile 1 and the deposited layer, following 2011-2012. Both D and Be have accumulated preferentially in regions where the surface of the W coating had local depressions due to the rough CFC surface.

Figure 4 shows an optical image, a topographical map and elemental maps from a region at position 0/3c following plasma operations 2011-2014. As evidenced by the topographical map and the W map, clearly the deposited layer has flaked off in a region on the right hand side, at some point during the operations. That region has the highest D areal density, in particular as regards the deeply trapped D. In fact, the flaked region carries most of the measured D in this region of the surface.

Figure 5 shows elemental maps from position 1/8, following operations 2013-2014. The fibre structure of the substrate in this case is perpendicular to the magnetic field, and is reflected in

the distributions of Be and D. The solid red lines indicate the approximate positions of major crests in the surface topography. This is also where the W signal is strongest. The Be and D distributions tend to be high to the left of the crests, with the Be slightly further away than the D from the crest.

4. Discussion

Of course it is not known precisely when in the operations history the arcing shown in Figure 2, or the flaking in Figure 4 occurred, but considering the significant deposition within the damaged regions it can not have happened at the very end of the campaigns. It is possible that the arcing and W erosion on Tile 0 is related to the W rich layer which was found in the deposited layers at nearby position 1/10 [15], in which case it should have happened at about one third into the operations campaign 2011-2012. It has been found previously that D and impurities tend to accumulate in small to moderately sized pits, cracks and other depressed regions of the vertical surfaces of the inner divertor [11-15]. In larger pits ($\sim 100 \mu\text{m}$) at the vertical surfaces in JET-ILW, the deposition has often occurred preferentially at some sides within pits [13,14]. In Figure 2 the surface D is found mainly at the centre of the larger arc spot. The Be is found slightly shifted to the left in the figure (inwards in JET). The deep D is found largely within the depressed region on the right, but also in the valley immediately to the right of the larger arc spot. The shift towards the left of the deposition maxima inside the large arc spot, as well as the maximum D accumulation on the right hand side of its rim could be related to the ion gyro motion being directed towards the left in the figure, but detailed modeling, such as in [16-18] is required to state anything conclusive.

The accumulation in substrate pits, as observed in Figure 3, is similar to what has been seen on the vertical surfaces of Tiles 1 and 3 in JET-ILW. In JET-C, it could be seen that D accumulated in pockets in the substrate at the vertical surfaces of Tile 1, whereas Be was enriched at the surface (Figure 3 of [12]), but that peculiar pattern was attributed to the chemical erosion of carbon.

The high D retention inside the area where the (mainly Be) deposited layer had flaked off is consistent with the general behaviour of preferential retention in depressed regions. However, this is a good example of where microanalysis improves the interpretation of analysis with poorer spatial resolution. The conclusion from broad beam analysis in this case would be that the D retention is associated with the intact deposited layer, whereas in fact most of the D in this particular area is trapped within the flaked region. Microanalysis in such cases opens the possibility to do reliable depth profiling in selected, relatively uniform surface areas [15].

Finally the deposition in regions with large scale ridges at the surface, as in Figure 5, shows systematic shadowing effects, which may likewise be suitable for modeling [16-18]. Efforts along these lines are in progress. It is at least clear that deposition in this situation occurs preferentially at specific slopes of the surface roughness, similar to what has been observed also at the sides of smaller pits at the vertical surfaces of Tiles 1 and 3 [13, 14]. It seems like this deposition at slopes occurs for smaller scale roughness on the vertical surfaces, compared to the upper, more horizontal surfaces, where generally the deposited layers are also thicker in JET-ILW.

5. Conclusions

Microanalysis of deposition and fuel retention at divertor surfaces has been extended to the horizontal surface of Tile 0, further out in the scrape-off layer and to the second operational period with JET-ILW. As with the vertical surfaces of Tiles 1 and 3, preferential deposition is found in pits at the surface, either in initial pits at the W coated surface, or in local depressed areas formed by damage (arcing and flaking). Preferential deposition at the sides of pits is also observed, but less prominently, compared to the vertical divertor surfaces. Examples are given where microanalysis can improve the interpretation of analysis with poorer spatial resolution.

References

- [1] J. Roth, E. Tsitrone, A. Loarte et al. *J. Nucl. Mater.* 390-391(2009)1-9.
- [2] J. Pamela, G. F. Matthews, V. Philipps et al. *J. Nucl. Mater.* 363(2007)1-11.
- [3] S. Brezinsek, A. Widdowson, M. Mayer et al. *Nucl. Fus.* 55(2015)063021.
- [4] M. Mayer, S. Krat, W. Van Renterghem et al. *Phys. Scr.* T167(2016)014051.
- [5] K. Heinola, A. Widdowson, J. Likonen et al. *Phys. Scr.* T167(2016)014075.
- [6] J. Likonen, K. Heinola, A. De Backer et al. *Phys. Scr.* T167(2016)014074.
- [7] I. Bykov, H. Bergsåker, G. Possnert et al. *Nucl. Instrum. Meth.* B371(2016)370-375.
- [8] D. Hildebrandt, H. Grote, W. Schneider et al. *Phys. Scr.* T81(1999)25-30.
- [9] A. Kreter, S. Brezinsek, T. Hirai et al. *J. Nucl. Mater.* 390-391(2009)1-8.
- [10] H. Khodja, C. Brosset, N. Bernier et al. *Nucl. Instrum. Meth.* B266(2008)1425-1429.
- [11] H. Bergsåker, P. Petersson, I. Bykov et al. *J. Nucl. Mater.* 438(2013)S668-S672.
- [12] H. Bergsåker, I. Bykov, P. Petersson et al. *Nucl. Instrum. Meth.* B332(2014)266-270.
- [13] I. Bykov, H. Bergsåker, P. Petersson et al. *Nucl. Instrum. Meth.* B342(2015)19-28.
- [14] H. Bergsåker, I. Bykov, P. Petersson et al. *J. Nucl. Mater.* 463(2015)956-960.
- [15] H. Bergsåker, I. Bykov, Y. Zhou et al. *Phys. Scr.* T167(2016)014061.
- [16] K. Schmid, M. Mayer, C. Adelhelm et al. *Nucl. Fus.* 10(2010)104004.
- [17] S. Dai, A. Kirschner, D. Mantev et al. *Plasm. Phys. Contr. Fus.* 55(2013)055004.
- [18] I. Bykov, H. Bergsåker and J. Likonen, Proc. 41st Eur. Conf. Plasm. Phys. Berlin, Germany, 23-27 June 2014.
- [19] M. Mayer, 2009 SIMNRA Users Guide 6-05, Max-Planck-Institut für Plasmaphysik, Garching, Germany. (<http://home.rzg.mpg.de/~mam/index.html>)

Figure captions.

Figure 1. Poloidal cross section of the upper part of the inner divertor, showing where samples have been taken. The Tile 0 samples had been exposed 2011-2012 and 2011-2014. The Tile 1 samples had been exposed 2013-2014.

Figure 2. Maps of a region of sample 0/2, exposed 2011-2012. Several arc tracks were found on this sample, where the W coating had been completely removed. Top left panel: proton spectrum showing how C, Be, surface D and deep D were separated. Top right: topographical map by optical focus stacking. Middle left: Carbon map. Middle right: Be map. Bottom left: surface D. Bottom right: deep D. The elemental maps are overlaid on an optical image.

Figure 3. Cross sections from position 1/10, following exposure 2011-2012. D and Be are both preferentially accumulated in pits at the surface of the W coating. The elemental maps are overlaid on an optical image.

Figure 4. Maps from position 0/3c, exposed 2011-2014, overlaid on an optical image. It is clear from the topographical map in the upper right panel and from the W map in the middle left that the deposited layer has flaked off at some point in the region to the right. The areal density of Be is consequently lower there, however the areal density of trapped D is larger in that region.

Figure 5. Maps from position 1/8, exposed 2013-2014. The vertical red lines indicate the positions of crests in the surface roughness, carried over through the W coating from the fibres of the CFC substrate. Preferential Be and D is observed between these crests, however not exactly at the same slopes of the surface roughness.

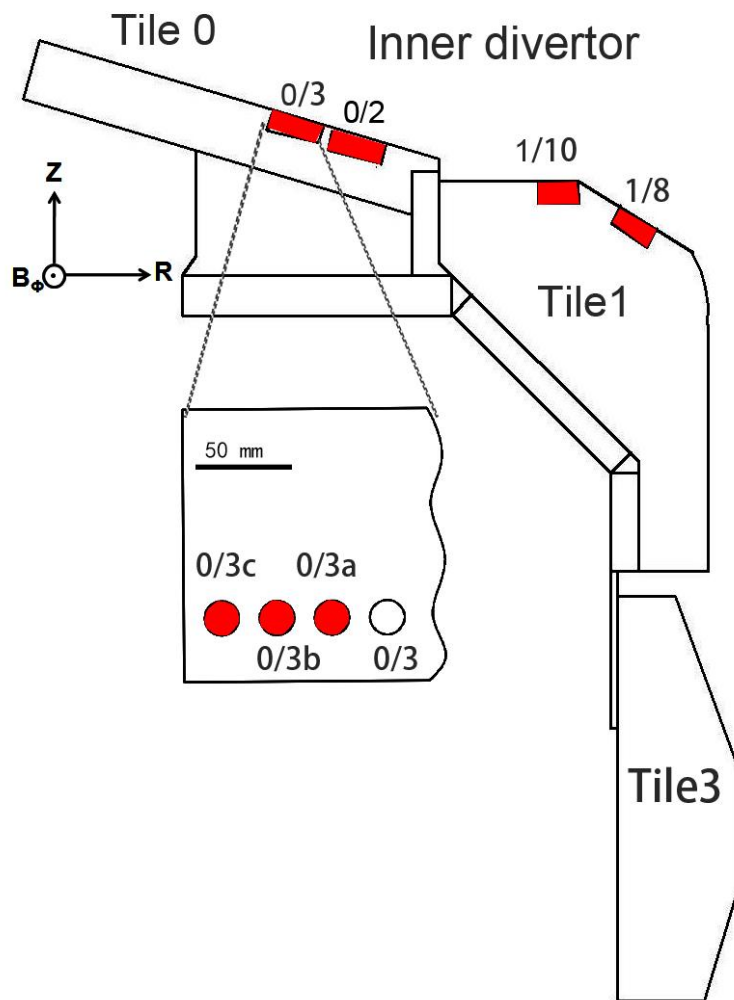


Figure 1. Poloidal cross section of the upper part of the inner divertor, showing where samples have been taken. The Tile 0 samples had been exposed 2011-2012 and 2011-2014. The Tile 1 samples had been exposed 2013-2014.

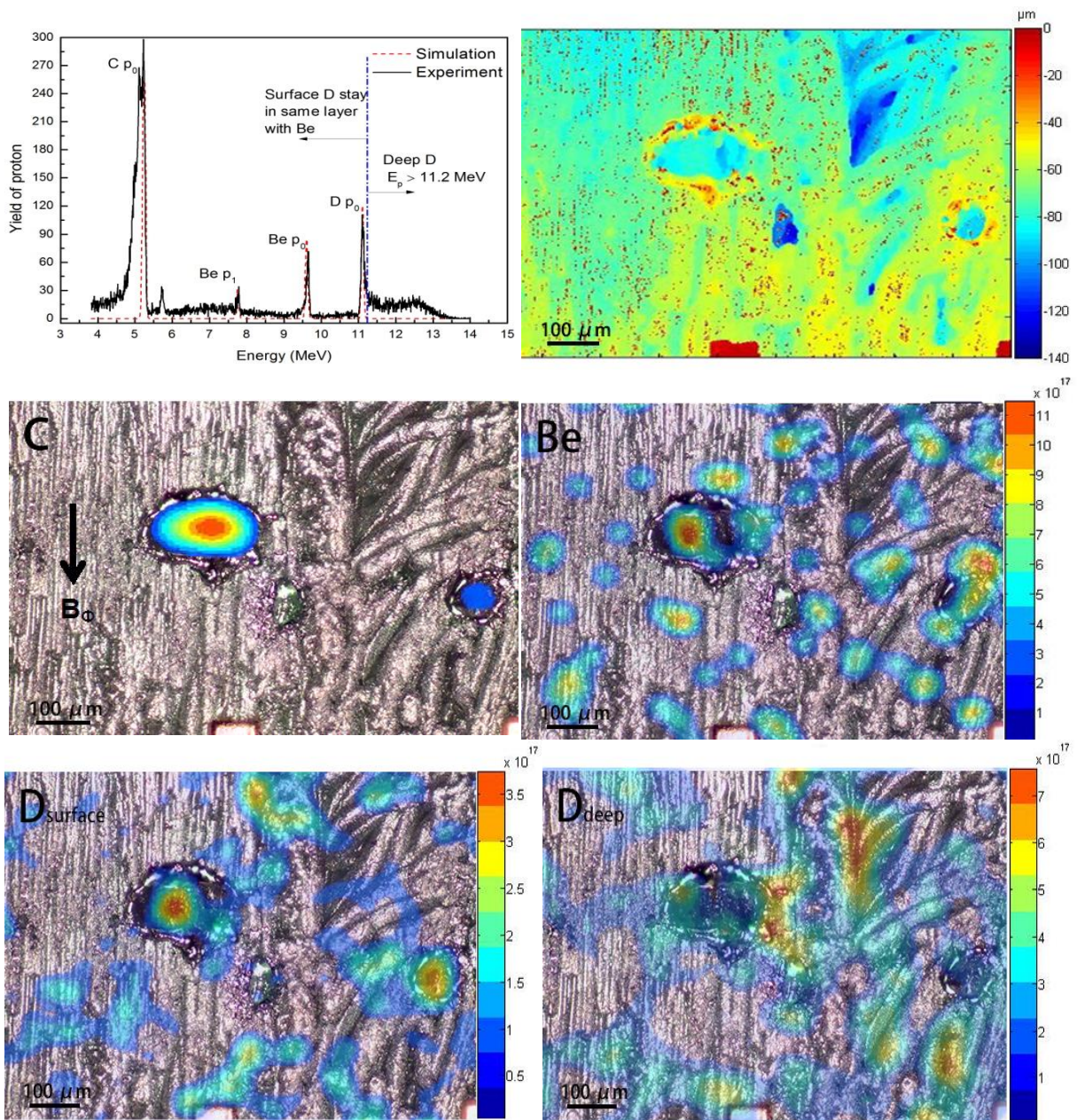


Figure 2. Maps of a region of sample 0/2, exposed 2011-2012. Several arc tracks were found, on this sample, where the W coating had been completely removed. Top left panel: proton spectrum showing how C, Be, surface D and deep D were separated. Top right: topographical map by optical focus stacking. Middle left: Carbon map. Middle right: Be map. Bottom left: surface D. Bottom right: deep D. The elemental maps are overlaid on an optical image.

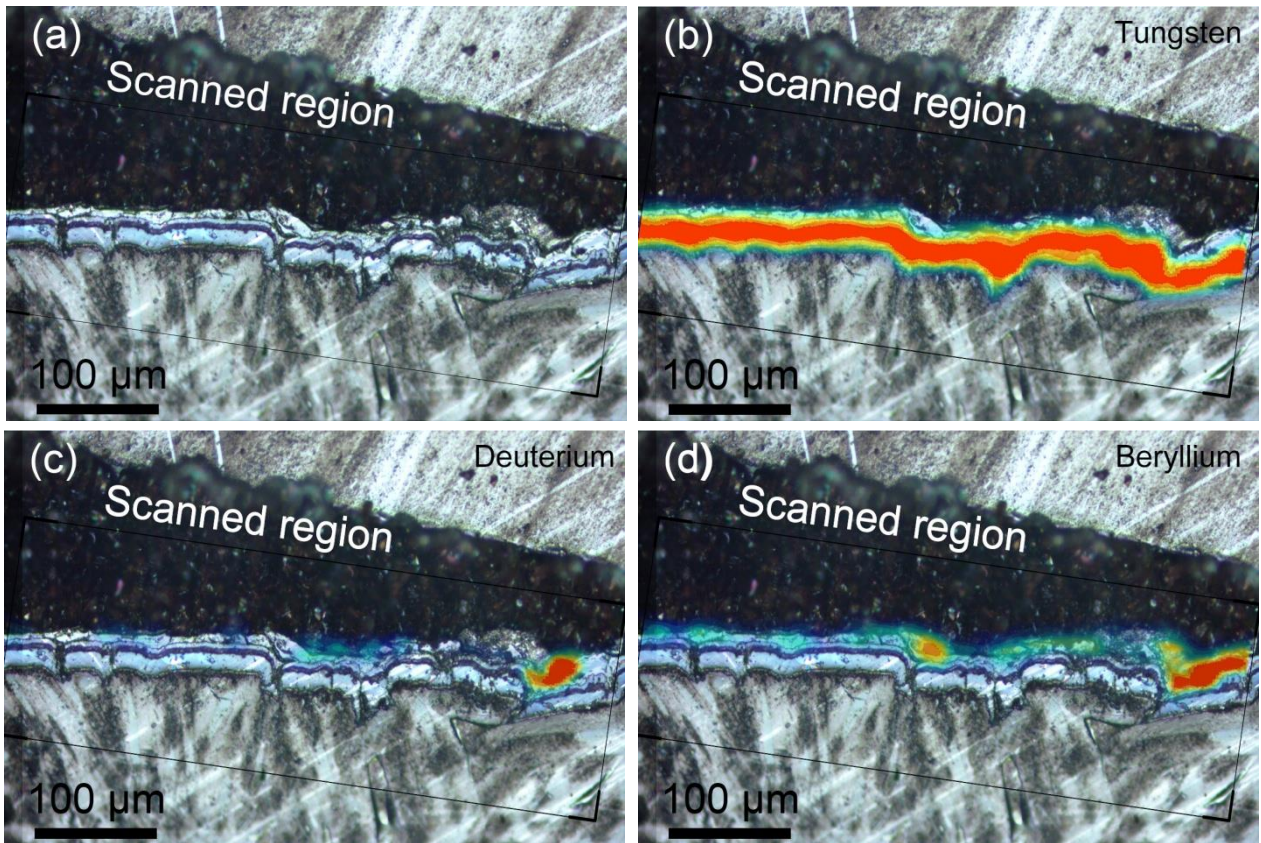


Figure 3. Cross sections from position 1/10, following exposure 2011-2012. D and Be are both preferentially accumulated in pits at the surface of the W coating. The elemental maps are overlaid on an optical image.

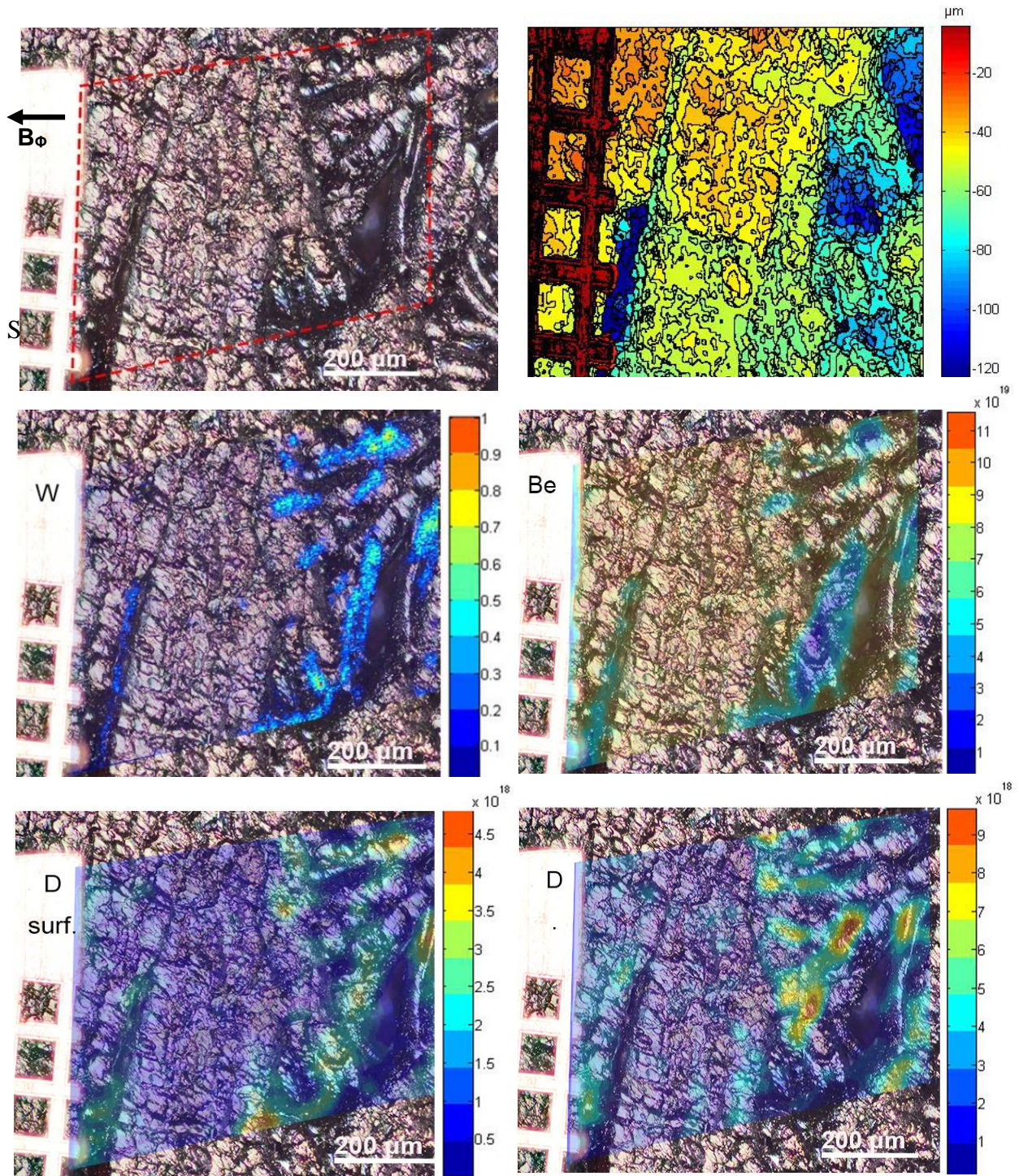


Figure 4. Maps from position 0/3c, exposed 2011-2014, overlaid on an optical image. It is clear from the topographical map in the upper right panel and from the W map in the middle left that the deposited layer has flaked off at some point in the region to the right. The areal density of Be is consequently lower there, however the areal density of trapped D is larger in that region.

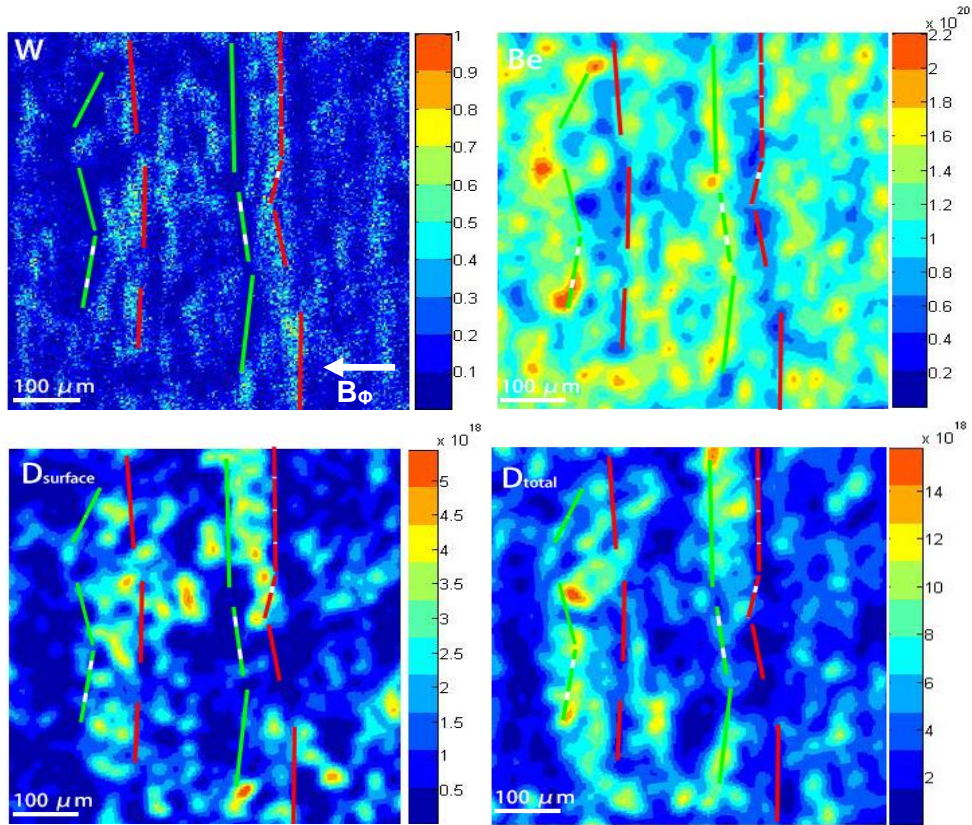


Figure 5. Maps from position 1/8, exposed 2013-2014. The vertical red lines indicate the positions of crests in the surface roughness, carried over through the W coating from the fibres of the CFC substrate. Preferential Be and D is observed between these crests, however not exactly at the same slopes of the surface roughness.

Sample	Period	Beryllium concentration (atoms/cm ²)	Deuterium concentration (atoms/cm ²)
0/2	2011-2012	$0.250 \cdot 10^{18}$	$0.284 \cdot 10^{18}$
0/3	2011-2014	$0.749 \cdot 10^{20}$	$0.279 \cdot 10^{19}$
1/8	2013-2014	$1.02 \cdot 10^{20}$	$0.405 \cdot 10^{19}$